HOKKAIDO UNIVERSITY

Title	Microscopic modulation of local density of states in superconducting alpha-(BEDT-TTF)(2)NH4Hg(SCN)(4) studied by site-selective C-13-NMR spectroscopy
Author(s)	Ihara, Y.; Noda, K.; Kawamoto, A.
Citation	Physical Review B, 90(4), 41107 https://doi.org/10.1103/PhysRevB.90.041107
Issue Date	2014-07-25
Doc URL	https://hdl.handle.net/2115/56911
Rights	©2014 American Physical Society
Type	journal article
File Information	PhysRevB_90_041107-.pdf

Hokkaido University Collection of Scholarly and Academic Papers : HUSCAP

PHYSICAL REVIEW B **90**, 041107(R) (2014)

Microscopic modulation of local density of states in superconducting α-(BEDT-TTF)$_2$NH$_4$Hg(SCN)$_4$ studied by site-selective ^{13}C-NMR spectroscopy

Y. Ihara,* K. Noda, and A. Kawamoto

Department of Physics, Graduate School of Science, Hokkaido University, Sapporo 060-0810, Japan

(Received 8 May 2014; revised manuscript received 13 July 2014; published 25 July 2014)

The local electronic state at every crystallographically independent molecular site was separately investigated in the organic superconductor α-(BEDT-TTF)$_2$NH$_4$Hg(SCN)$_4$ using site-selective ^{13}C-NMR spectroscopy. The density of states (DOS) at three molecular sites shows independent temperature variation, which is caused by the long-range Coulomb interaction. Comparing the present results with those for a nonsuperconducting counterpart α-(BEDT-TTF)$_2$RbHg(SCN)$_4$, we found that the uniform DOS at two of three independent molecular sites is crucial to induce superconductivity. Taking the site-dependent DOS as a parameter, we constructed a phase diagram for a superconductor with long-range Coulomb interaction, an α-type BEDT-TTF family, and summarized the competition between charge instability and superconductivity.

DOI: 10.1103/PhysRevB.90.041107 PACS number(s): 74.25.nj, 74.70.Kn, 75.25.Dk

Unconventional superconductivity has been frequently found after the suppression of the order in the spin degrees of freedom. Properties of unconventional superconductivity near magnetic order have been intensively studied since the discovery of heavy fermion and cuprate superconductors. In these systems, superconductivity is induced by magnetic critical fluctuations enhanced near the second-order phase transition. The organic superconductors (TMTSF)$_2X$ (TMTSF: tetramethyltetraselenafulvalene) and κ-(BEDT-TTF)$_2X$ (BEDT-TTF: bisethylenedithio-tetrathiafulvalene) are also categorized by magnetic-fluctuation-induced superconductivity [1,2]. In some BEDT-TTF salts, however, superconductivity was found near the order in the charge degrees of freedom. One of the most intensively studied examples is the α-(BEDT-TTF)$_2X$ family, in which superconductivity appears after suppressing charge instability by chemical substitution or application of mechanical pressures [3–6]. Theoretical studies have suggested that superconducting (SC) pairs can be mediated by critical charge fluctuations near the charge ordering (CO), which is caused by a sizable off-site Coulomb repulsion [7]. The properties of superconductivity near charge instability should be investigated to understand the diversity of SC pairing mechanisms.

To reveal the relationship between superconductivity and charge instability, a phase diagram for various α-type BEDT-TTF salts has been proposed [5]. In this phase diagram, the ratio of lattice parameters c/a was used as the tuning parameter, which modifies the anisotropy of the transfer integrals in the conduction (ac') plane. Among the α-(BEDT-TTF)$_2X$ salts, a clear CO transition at $T_{CO} = 135$ K was reported in α-(BEDT-TTF)$_2$I$_3$ (I$_3$ salt) with $c/a \simeq 0.85$ [8]. The uniaxial strain along the c direction decreases the c/a ratio to induce superconductivity with the transition temperature T_c reaching 7 K [4]. The resistivity in c axial strain shows semiconducting behavior before the SC transition, while a axial strain induces metallic resistivity down to the lowest temperature without a SC transition. In another α-type salt, α-(BEDT-TTF)$_2$NH$_4$Hg(SCN)$_4$ (NH$_4$ salt) with a larger c/a ratio of 0.987, metallic resistivity was observed in the entire temperature range, and superconductivity appears even at ambient pressure below $T_c = 1$ K [9], which can be increased up to 6 K by c axial strain [5]. Besides, α-(BEDT-TTF)$_2$KHg(SCN)$_4$ (K salt) with the largest c/a ratio of 0.99 demonstrates two charge anomalies at $T_{CDW} = 8$ K [10] and $T^*_{CO} \simeq 200$ K [11–13]. In K salt, superconductivity can be induced by the application of hydrostatic pressures [14,15]. The previously proposed c/a phase diagram thus cannot explain the variation of the electronic properties in the normal state, and the relationship between CO and SC phases. To universally understand the SC, CO, and charge-density-wave (CDW) states in α-(BEDT-TTF)$_2X$, electronic states should be summarized in a phase diagram, for which a parameter directly connected to the electronic state is used as the horizontal axis.

The lattice constants are not the best parameters because the band structure is determined by a combination of transfer integrals between three crystallographically independent BEDT-TTF molecules A, B, and C. In the conduction plane of α-type packing, two A molecules are connected with inversion symmetry, and the B and C molecules locate on the inversion center, as shown in Fig. 1(a). The A molecules and B,C molecules stack along the c direction to form a columnar structure, and the A and B-C columns alternate along the a direction. Despite the columnar structure along the c direction, band calculation suggested a quasi-one-dimensional (1D) Fermi sheet perpendicular to the a direction in K, Rb, and NH$_4$ salts [16], which results in the highest conductivity along the a direction. In addition to the 1D Fermi sheet, α-(BEDT-TTF)$_2X$ salts also possess a two-dimensional (2D) Fermi surface. As the local transfer integrals for every site are responsible for the determination of band structure, we should utilize a parameter that directly reflects the local electronic states to construct the phase diagram.

The crystal and band structures of K salt are similar to those of NH$_4$ salt. In the ground state, however, NH$_4$ salt shows superconductivity, while K salt shows a CDW state, which was found as a small hump on the metallic conductivity [10]. The difference in normal-state electronic properties would lead us to reveal the origin of SC pair formation. The high-temperature electronic properties in K and NH$_4$ salts have been investigated

*yihara@sci.phys.hokudai.ac.jp

 ©2014 American Physical Society

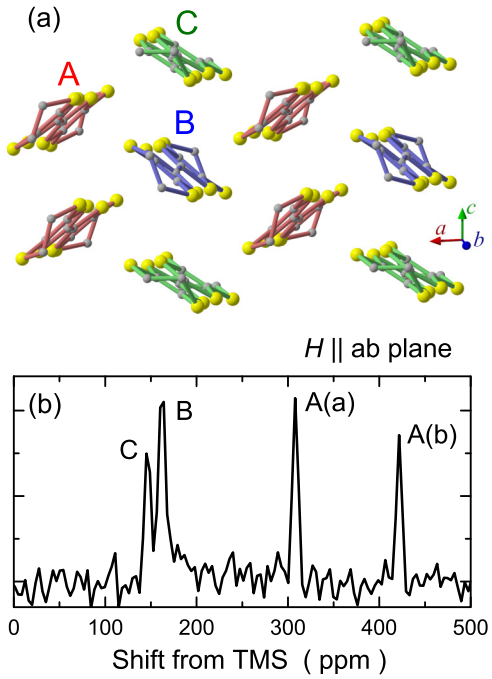


FIG. 1. (Color online) (a) Molecular arrangement of α-(BEDT-TTF)$_2$NH$_4$Hg(SCN)$_4$ in the conduction plane. Three crystallographically independent molecules A, B, and C form the A and B-C columns along the c direction. (b) The ^{13}C-NMR spectrum obtained at room temperature. The observed four separate peaks were assigned to each ^{13}C site, as denoted in the figure from the angle-resolved NMR measurement. A(a) and A(b) are two independent ^{13}C sites on the A molecule.

from optical and x-ray diffraction measurements. In K salt, the x-ray diffraction measurement detected diffuse scattering associated with CDW coherence below $T_{CO}^{*} \simeq 200$ K [12,17]. At a corresponding temperature, the pseudogap behavior was observed in the optical conductivity, and was attributed to the effect of critical charge fluctuation [11]. This charge fluctuation would be related to the SC pairing mechanism in α-type salts. However, the pseudogap behavior is masked by a dominant Drude contribution in SC NH$_4$ salt. Similar pseudogap behavior was clearly observed in the optical conductivity for β''-type superconductors with charge instability near β''-(BEDT-TTF)$_2$SF$_5$CH$_2$CF$_2$SO$_3$ [18]. By comparing the results for the non-SC counterpart β''-(BEDT-TTF)$_2$SO$_3$CHFSF$_5$, Kaiser *et al.* suggested the importance of charge fluctuations for SC pair formation. The charge fluctuation in NH$_4$ salt should be investigated to attest the charge-fluctuation scenario for superconductivity in α-type BEDT-TTF members.

The high-temperature charge instability at T_{CO}^{*} has been studied by the site-selective ^{13}C-NMR experiment on α-(BEDT-TTF)$_2$RbHg(SCN)$_4$ (Rb salt), which shows essentially identical electronic properties with K salt, except for a slightly high $T_{CDW} = 10$ K. Although the ^{13}C-NMR experiment is sensitive only to the magnetic properties, the broadening of the ^{13}C-NMR spectrum due to static charge modulation was observed at the A site below $T_{CO}^{*} \simeq 200$ K [13]. This result is consistent with weak intracolumn charge modulation on the A column detected by infrared spectroscopy at a corresponding temperature [19]. As we have confirmed that the NMR linewidth can detect the local charge instability, the effect of charge instability on superconductivity should be explored in NH$_4$ salt using a site-selective NMR measurement. However, a NMR study on NH$_4$ salt was performed only on the polycrystal [20].

In this Rapid Communication, we measured the ^{13}C-NMR signal on the single crystalline α-(BEDT-TTF)$_2$NH$_4$Hg(SCN)$_4$ salt, which was grown by the electrochemical oxidation technique. ^{13}C was selectively enriched for one side of the central C = C bond [21]. The asymmetrically ^{13}C enriched molecule eliminates the NMR spectral splitting due to nuclear spin-spin coupling at the C = C bond (Pake doublet) [22], and enables us to execute an unambiguous site assignment even for a complicated α structure with three independent BEDT-TTF molecules. The nuclear spin-lattice relaxation rate T_1 was measured at each line using the conventional saturation-recovery method. We applied an external magnetic field of 9.4 T to the direction, for which four NMR lines are sufficiently separated.

As shown in Fig. 1(b), the ^{13}C-NMR spectrum consists of four NMR signals from four independent ^{13}C sites. According to the site symmetry, B and C molecules possess only one ^{13}C site at the central C = C bond, and the A molecule has two nonequivalent ^{13}C sites. The four NMR lines were assigned to each ^{13}C site on the basis of an angle resolved NMR experiment [23].

Figure 2(a) shows the static susceptibility measured at each molecular site. The details of the analysis to derive site-selective spin susceptibility from NMR shift data are presented in the Supplemental Material [23]. A spin disproportion between the A and B-C column exists already at room temperature, and the disproportion between B and C molecules develops at low temperatures. This behavior resembles the site-dependent susceptibility for Rb salt, which is shown as the open symbols in Fig. 2(a) [13]. The susceptibility of A and B sites χ_A and χ_B for NH$_4$ salt deviates from those for Rb salt below 100 K. A continuous increase in χ_A and χ_B suggests a larger density of states (DOS), which would be essential to suppress the CDW state and induce superconductivity at low temperatures. Contrastingly, susceptibility of the C site χ_C decreases to a small value in both salts. As the static electronic properties for the C site are identical between NH$_4$ and Rb salts, and the contribution of electrons at the C molecule to the Fermi surface is small, the difference in the ground state should be raised from the electrons at other sites.

The charge disproportionation between the B and C sites indicates that the electronic state in NH$_4$ salt is affected by a strong off-site Coulomb interaction. We explored the high-temperature charge instability on the A column from the NMR spectrum for the A site, and observed an increase in linewidth below $T_{CO}^{*} \simeq 180$ K, as shown in Fig. 2(b). This linewidth broadening suggests that the SC NH$_4$ salt exhibits the same weak CO on the A column as those observed in Rb and K salts. As the collective charge excitation observed in K salt is related to this high-temperature CO [11], we suggest the relationship between charge excitations and the SC pairing mechanism in NH$_4$ salt.

To figure out the origin of superconductivity that is induced in NH$_4$ salt, we have measured the nuclear spin-lattice

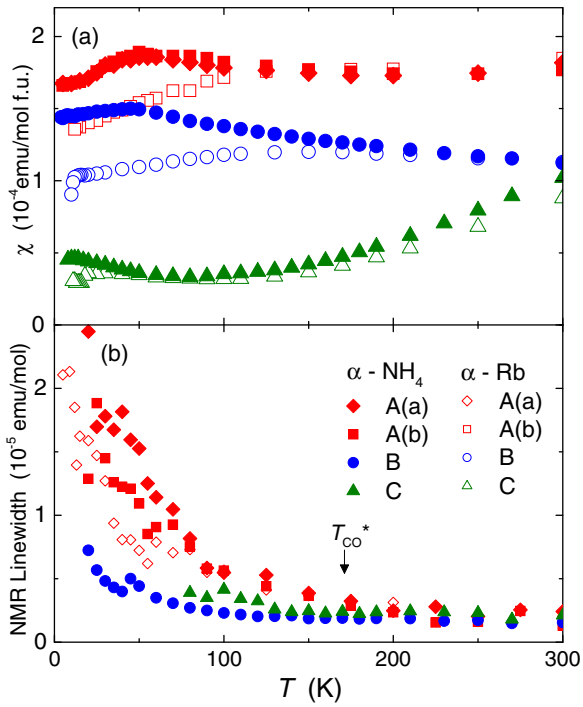


FIG. 2. (Color online) (a) Temperature dependence of local spin susceptibility at each site in NH_4 salt (solid symbols) and Rb salt (open symbols [13]). The same symbols for each ^{13}C site were used throughout this work. The difference in static susceptibility between NH_4 and Rb salts was observed only below 100 K. (b) The NMR linewidth determined at each peak. The line broadening at A sites below 180 K indicates that the charge instability reported in Rb salt exists also in the SC NH_4 salt.

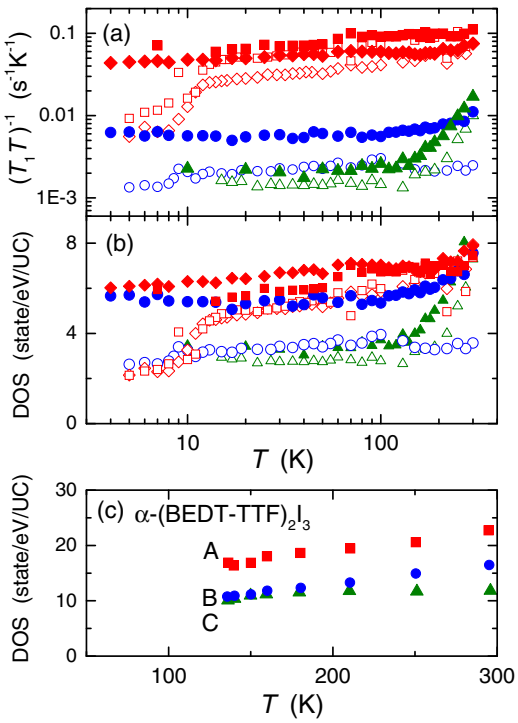


FIG. 3. (Color online) (a) Temperature dependence of $(T_1T)^{-1}$ measured at each ^{13}C site. The results for Rb salt (open symbols) are displayed together for comparison [24]. The temperature-independent Fermi liquid behavior was observed between 4 and 100 K. (b) Local DOS for each site estimated using Eq. (1) (see text). The DOS at the A and B sites becomes almost equivalent at low temperatures in NH_4 salt, while in Rb salt the DOS of the B site decreases to the values of the C site. (c) The local DOS for α-$(BEDT\text{-}TTF)_2I_3$ at ambient pressure [25]. The DOS at the B site is comparable to that at the C site. The low-temperature data below 135 K were not obtained due to a CO transition.

relaxation rate $1/T_1$ at each molecular site, and estimated the local DOS. In Fig. 3(a), $1/T_1T$ measured at each ^{13}C site is displayed together with the results for Rb salt. We note that $1/T_1T$ at the C site becomes small for both salts, in accordance with the static susceptibility results. The small values of $1/T_1T$ at the C site suggest that the electrons at the C molecules hardly contribute to the electronic properties. The temperature dependence observed above 200 K at the C site is ascribed to the slow molecular dynamics, which does not directly couple to the conduction electrons.

When electron-electron correlations are weak enough not to violate the Fermi liquid state, $1/T_1T$ is written as

$$\frac{1}{T_1T} = \frac{4\pi k_B}{\hbar} A_{\rm hf}^2 N(E_{\rm F})^2, \qquad (1)$$

where $N(E_{\rm F})$ is the DOS at the Fermi energy. The hyperfine coupling constant $A_{\rm hf}$ is expressed using the hyperfine field $H_{\rm hf}$ and gyromagnetic ratio γ_n as $A_{\rm hf} = \gamma_n \hbar H_{\rm hf}/N$. The temperature-independent Fermi liquid behavior observed at all sites below 100 K confirms that magnetic excitations near magnetic instability are absent in this salt. We can exclude the magnetic scenario for SC pair formation. In the Rb salt, $1/T_1T$ decreases abruptly below 12 K due to the CDW transition, while NH_4 salt is in the Fermi liquid state down to the lowest temperature measured (4 K). The DOS at the Fermi surface vanishes in the CDW state, and becomes comparable to the value for the C site, which confirms the small local DOS at the C site.

In the normal state above 12 K, the absolute value of $1/T_1T$ for the B site is significantly different between NH_4 and Rb salts. The local DOS at each site was determined by using Eq. (1) and the results of $1/T_1T$. Details of the analyses to determine $A_{\rm hf}$ for each site is presented in the Supplemental Material [23]. As shown in Fig. 3(b), the local DOS for the B site is significantly different between SC and non-SC salts. In NH_4 salt, the local DOS for the A and B sites converges to a single value at the lowest temperature, while in Rb salt, the DOS at the B site goes toward a value that is as small as that for the C site. The site-selective χ measurement also yields a similar result, that is, a uniform DOS at the A and B sites for NH_4 salt, and a nonuniform DOS for Rb salt. It is worth noting that static susceptibility at high temperature ($T >$ 150 K) shows the same behavior between NH_4 and Rb salts. We suggest that the low-temperature electronic state should be investigated to reveal the SC mechanisms in α-type BEDT-TTF salts.

In addition to the NH_4 and Rb salts, we analyzed the electronic state in I_3 salt at ambient pressure. The local DOS at each molecular site can be estimated by applying the present

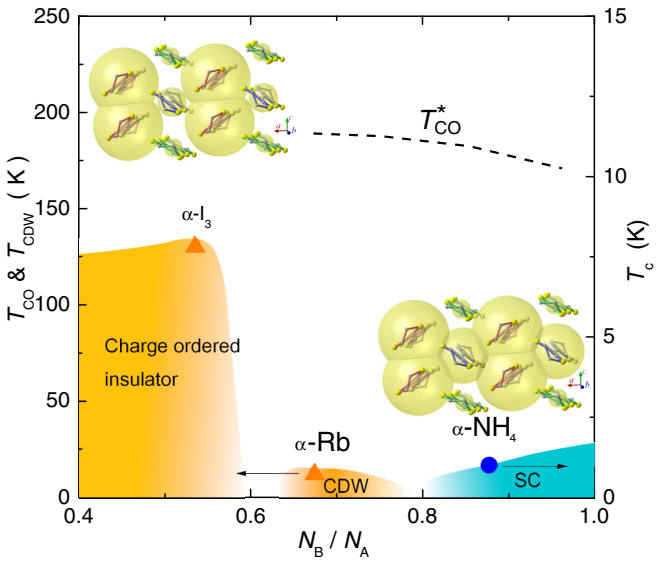


FIG. 4. (Color online) A phase diagram for α-type BEDT-TTF salts. The ratio between local DOS at B and A sites N_B/N_A was used as the horizontal axis. This ratio parametrizes the homogeneity of local DOS along the a direction. In this phase diagram, the charge ordered state in I_3 and Rb salts appears on the same side of the SC state. The crystal structure in the figure denotes a schematic image of the local DOS at each molecular site.

analyses to the published data [25]. Even though the absolute values are different from those in NH_4 and Rb salts because of the difference in band structure, we can clearly conclude that the local DOS at the B site is much smaller than that at the A site, and comparable to the value for the C site, as shown in Fig. 3(c). We confirmed from the site-selective NMR experiment on three different salts that SC salt has a uniform DOS between the A and B sites while non-SC salts have large inhomogeneity. This qualitative difference between the SC and non-SC α salts will add an important constraint on the theoretical model.

As it has been revealed that a uniform DOS is required to induce superconductivity, we depict a phase diagram in Fig. 4, taking the ratio of DOS at the B and A sites N_B/N_A as the tuning parameter. In this phase diagram, I_3 and Rb salts with charge instability are both on the left side of the SC phase. From the ambient pressure results on three α-type salts, we suggest that N_B/N_A is a useful parameter to understand the relationship between charge instability and superconductivity. On the basis of this phase diagram, we speculate that the a axial strain on I_3 salt would increase the local DOS at the B site, which results in metallic conductivity [4]. The site-selective ^{13}C NMR experiment under uniaxial strain is now in progress. The modification of the band structure by c axial strain and hydrostatic pressure brings I_3 salt away from Rb and NH_4 salts, so as to induce a semiconducting state and a Dirac electron state, respectively.

Now, we discuss a possible interpretation for the tuning parameter N_B/N_A. The ratio close to unity indicates a uniform electronic state at the A and B molecules, that is, the electronic wave function expands toward the a direction to increase the transfer integrals. As the high conductivity along the a direction is associated with the 1D Fermi sheet, the uniform DOS at the A and B sites could be related to the 1D Fermi sheet. In fact, as the 1D Fermi sheet is absent in I_3 salt, the local DOS is most strongly modulated along the a direction. These results suggest the importance of the 1D Fermi sheet in addition to the collective charge excitations on the A column to realize superconductivity.

In summary, we have performed a site-selective ^{13}C-NMR experiment on SC NH_4 salt, and revealed that the A column shows a weak charge modulation below 180 K, as was observed in Rb salt with a CDW ground state. We also confirmed that magnetic excitations near magnetic instability are absent in NH_4 salt from the $1/T_1T$ measurement. These results suggest a possibility that superconductivity in NH_4 salt is induced by charge fluctuations, in accord with optical conductivity measurements. In addition to the observation of charge instability at high temperature, we found that the large local DOS at the B molecule is crucial to induce superconductivity, which addresses the importance of the 1D Fermi sheet. We depicted a phase diagram taking N_B/N_A as the tuning parameter, and summarized the SC, CO, and CDW states observed in α-type BEDT-TTF salts. This phase diagram could be compared to the theoretical calculations, and will help understand superconductivity near charge instability.

The authors would like to thank N. Matsunaga for useful discussion. This work was partially supported by MEXT KAKENHI Grants No. 25610082 and No. 24540353.

[1] D. Jerome, A. Mazaud, M. Ribault, and K. Bechgaard, J. Phys. (Paris) Lett. **41**, 95 (1980).

[2] J. M. Williams, A. J. Schultz, U. Geiser, K. D. Carlson, A. M. Kini, H. H. Wang, W.-K. Kwok, M.-H. Whangbo, and J. E. Schirber, Science **252**, 1501 (1991).

[3] N. Kinoshita, M. Tokumoto, and H. Anzai, J. Phys. Soc. Jpn. **60**, 2131 (1991).

[4] N. Tajima, A. Ebina-Tajima, M. Tamura, Y. Nishio, and K. Kajita, J. Phys. Soc. Jpn. **71**, 1832 (2002).

[5] M. Maesato, Y. Kaga, R. Kondo, and S. Kagoshima, Phys. Rev. B **64**, 155104 (2001).

[6] D. Andres, M. V. Kartsovnik, W. Biberacher, K. Neumaier, and H. Müller, J. Phys. IV (France) **12**, 87 (2002).

[7] J. Merino, and R. H. McKenzie, Phys. Rev. Lett. **87**, 237002 (2001).

[8] K. Bender, I. Henning, D. Schweitzer, K. Dietz, H. Endres, and H. J. Keller, Mol. Cryst. Liq. Cryst. **108**, 359 (1984).

[9] H. H. Wang, K. D. Carlson, U. Geiser, W. K. Kwok, M. D. Vashon, J. E. Thompson, N. F. Larsen, G. D. Mccabe, R. S. Hulscher, and J. M. Williams, Physica C **166**, 57 (1990).

[10] T. Sasaki and N. Toyota, Solid State Commun. **75**, 93 (1990).

[11] M. Dressel, N. Drichko, J. Schlueter, and J. Merino, Phys. Rev. Lett. **90**, 167002 (2003).
[12] P. Foury-Leylekian, J.-P. Pouget, Y.-J. Lee, R. M. Nieminen, P. Ordejón, and E. Canadell, Phys. Rev. B **82**, 134116 (2010).
[13] K. Noda, Y. Ihara, and A. Kawamoto, Phys. Rev. B **87**, 085105 (2013).
[14] D. Andres, M. V. Kartsovnik, W. Biberacher, K. Neumaier, E. Schuberth, and H. Müller, Phys. Rev. B **72**, 174513 (2005).
[15] M. V. Kartsovnik, W. Biberacher, D. Andres, S. Jakob, M. Kunz, N. Neumaier, H. Müller, and N. D. Kushch, Physica B **407**, 1919 (2012).
[16] H. Mori, S. Tanaka, M. Oshima, G. Saito, T. Mori, Y. Maruyama, and H. Inokuchi, Bull. Chem. Soc. Jpn. **63**, 2183 (1990).
[17] P. Foury-Leylekian, S. Ravy, J.-P. Pouget, and H. Müller, Synth. Met. **137**, 1271 (2003).
[18] S. Kaiser, M. Dressel, Y. Sun, A. Greco, J. A. Schlueter, G. L. Gard, and N. Drichko, Phys. Rev. Lett. **105**, 206402 (2010).
[19] T. Hiezima, S. Yamada, M. Uruichi, and K. Yakushi, Physica B **405**, S153 (2010).
[20] K. Miyagawa, A. Kawamoto, and K. Kanoda, Synth. Met. **86**, 1987 (1997).
[21] M. Yamashita, A. Kawamoto, and K. Kumagai, Synth. Met. **133–134**, 125 (2003).
[22] G. E. Pake, J. Chem. Phys. **16**, 327 (1948).
[23] See Supplemental Material at http://link.aps.org/supplemental/10.1103/PhysRevB.90.041107 for technical details of NMR data analyses.
[24] T. Kawai and A. Kawamoto, J. Phys. Soc. Jpn. **78**, 074711 (2009).
[25] S. Hirose and A. Kawamoto, Phys. Rev. B **82**, 115114 (2010).